

Statistical Analysis for Projected Exoplanet Quantities

Robert A. Brown

Space Telescope Science Institute, 3700 San Martin Drive, Baltimore, MD 21218

rbrown@stsci.edu

ABSTRACT

Exoplanet searches using radial velocity (RV) and microlensing (ML) produce samples of “projected” mass and orbital radius, respectively. We present new methods for inferring the underlying distributions of the true, unprojected quantities from such samples. From the inferred distribution, we define random deviates for the projected quantities, which we use in Monte Carlo experiments to investigate the accuracy of the inferred distribution. For illustration, we apply the methods to all 308 current values of projected mass from radial-velocity searches, as well as a sample 67 values given a similar treatment by Jorissen et al. in 2001, with which we compare our results. In addition to analyzing observational results, our methods can be used to develop measurement requirements for future programs, such as the microlensing survey of Earth-like exoplanets recommended by the Astro 2010 committee. Our simple experiments with RV samples suggest that samples of thousands of observed values of the projected quantities are needed for believable conclusions about the basic shape of the underlying distributions of unprojected quantities in the operating regimes of current RV and ML programs.

Subject headings: astrobiology – methods: analytical – methods: data analysis – methods: statistical – techniques: radial velocity – (stars:) planetary systems – (stars:) binaries: spectroscopic

1. INTRODUCTION

Mass m and orbital radius r are two key factors for the habitability of exoplanets. This is because m plays an important role in the retention of an atmosphere, and r is a key determinant of the surface temperature. Besides those connections to the cosmic search for life, the true distributions of m and r are also important for theories of the formation and dynamical evolution of planetary systems. Therefore, we have a variety of good reasons to

better understand the distributions of m and r . Such improvement will involve learning more from measurements already made, as well as anticipating future results, from telescopes and observing programs of the future.

We focus on two techniques that measure projected quantities. One is radial velocity (RV), the source of many exoplanet discoveries so far. The other is a microlensing (ML). Astro 2010 recently recommended a ML survey for Earth-mass exoplanets on orbits wider than detectable by *Kepler* (Blandford et al. 2010). One goal of this paper is to introduce a new class of science metrics for the ML survey, and to demonstrate their use with existing RV results. Such science metrics will be useful for setting measurement requirements, designing telescopes and instruments, planning science operations, and arriving at realistic expectations, especially for the new ML survey program.

RV yields the unprojected value of r , from the orbital period, but for mass it can only provide $m \sin i$ —not m —where i is the usually unknown orbital inclination angle. ML yields m —if the stellar mass is known or assumed—but for r it usually can provide only $r \sin \beta$ —not r —where β is the usually unknown planetocentric angle between the star and observer (Bennett 2009). Even when the projection angle is unknown, we can use statistical methods to draw inferences about the distribution of the true values from samples of the projected values. This paper presents new methods to help draw those inferences, which should also provide a framework for ongoing statistical, science-metrical studies of RV and ML projected quantities.

2. STARTING POINT

Our starting point is recognizing that a projected property— $m \sin i$ or $r \sin \beta$ —is the product of two continuous, independent random variables. The distribution of such a product is a function of the distributions of the two variables. The distribution of the first factor— m or r —is what we want to learn about, from nature. The second, the angular factor $\sin i$ or $\sin \beta$ —for which we introduce the variable y —is distributed uniformly on the sphere, with probability density function (PDF):

$$\mathcal{Q}(y) = \frac{y}{\sqrt{1-y^2}} \quad , \quad (1)$$

where the projection angles are in the interval $0-\pi$, and y is in the interval $0-1$.

We introduce two more generic symbols: $u \equiv \log(m \sin i)$ or $\log(r \sin \beta)$ with PDF $\mathcal{P}(u)$, and $x \equiv \log m$ or $\log r$ with PDF $\mathcal{R}(x)$. (The logarithmic variables are preferred due to the wide dynamic range—almost four decades in the case of RV exoplanets.) Using these

definitions, we can write

$$\mathcal{P}(u) = \mathcal{C}(u) \ln 10 \int_u^\infty \mathcal{R}(x) \mathcal{Q}(10^{u-x}) 10^{u-x} dx \quad , \quad (2)$$

where we have made use of the theorem of Glen, Leemis, & Drew (2004) for the PDF of the product of random variables, and have changed to logarithmic variables. \mathcal{C} is the completeness function, to account for variations in instrumental sensitivity with u , for example, and perhaps other selection effects due to the instrument, observations, or analysis. In the absence of such effects, $\mathcal{C}(u) \equiv 1$.

We recognized that Eq. (2) has a thought-provoking analogy to the case of an astronomical image (which corresponds to \mathcal{P}), where the object (\mathcal{R}) is convolved with the telescope’s point-spread function (\mathcal{Q}) and the field is, say, vignetted in the camera (\mathcal{C}). Pursuing this analogy, we might call the form of the integral in Eq. (2) “logarithmic convolution.” It could be said that we “see” the true distribution (\mathcal{R}) only after it has been logarithmically convolved with the projection function (\mathcal{Q}) and modulated by the completeness function (\mathcal{C}). As with image processing, we can correct “vignetting” by dividing \mathcal{P} by \mathcal{C} , if we know it, and then “deconvolve” the result to remove the effects of \mathcal{Q} —which in this case we know *exactly*. As with image processing, the result can be a transformation—a new, alternative, precise description of the sample, in the form of an estimate of the “object”—the natural distribution \mathcal{R} —with some systematic effects removed (but other effects, possibly remaining).

Equation (2) is a form of Abel’s integral equation, as discussed in this general context by Chandrasekhar & Münch (1950), who used the formal solution to investigate the distribution of true and apparent rotational velocities of stars. Later, Jorissen et al. (2001) inferred the distribution of exoplanet masses from 67 values of $m \sin i$, using both the formal solution and the Lucy-Richardson algorithm. We present a third numerical approach to solve Eq. (2), and emphasize the follow-on applications afforded by the derived random deviates.

In Section 3, we develop the new methods for transforming samples of measured values $\{u_i\}$ of a projected property into empirical distributions for the unprojected quantity. In Section 4, we demonstrate these computations on a sample of RV results—the 308 values of $m \sin i$ available at exoplanets.org on 20 October 2010. In Section 5, we develop random deviates for use in Monte Carlo experiments. In Section 6, we illustrate how the accuracy of inferences depends on the cardinality of the sample. Here, we treat both the current sample of 308 RV values and an earlier sample of 67 values treated by Jorissen et al. (2001). In Section 7, we comment on implications and future directions.

3. NEW METHODS

We assume the sample of projected values $\{u_i\}$ is non-redundant and sorted in ascending order. The cardinality is n . The empirical cumulative distribution function (CDF) for u is

$$\hat{P}(u) \equiv \frac{1}{n} \sum_{i=1}^n \mathcal{I}(u_i \leq u) \quad , \quad (3)$$

where \mathcal{I} is the indicator function

$$\mathcal{I}(\text{logical statement}) \equiv 1 \text{ if the statement is true and } 0 \text{ otherwise} \quad . \quad (4)$$

\hat{P} estimates the true CDF of the projected quantity, which is

$$P(u) \equiv \int_{-\infty}^u \mathcal{P}(u') du' \quad . \quad (5)$$

Assume that the completeness function is unity ($\mathcal{C}(u) \equiv 1$) or has been corrected (i.e., $\hat{P}(u)$ now means $\hat{P}(u)/\mathcal{C}(u)$).

We can approximate \mathcal{R} by a sum of Dirac delta functions at N points $\{x_j\}$ with weights $\{w_j\}$:

$$\mathcal{R}(x) \simeq \hat{\mathcal{R}}(x) \equiv \sum_{j=1}^N w_j \delta(x - x_j) \quad . \quad (6)$$

The associated approximation of $P(u)$ is

$$\begin{aligned} P(u) \simeq \hat{P}'(u) &\equiv \int_{-\infty}^u \ln 10 \int_{u'}^{\infty} \sum_{j=1}^N w_j \delta(x - x_j) Q(10^{u'-x}) 10^{u'-x} dx du' \quad (7) \\ &= \sum_{j=1}^N w_j \ln 10 \int_{-\infty}^u \frac{10^{2(u'-x_j)}}{\sqrt{1 - 10^{2(u'-x_j)}}} \mathcal{H}(-u' + x_j) du' \\ &= \sum_{j=1}^N w_j \left(1 - \sqrt{1 - 10^{2(u-x_j)}} \mathcal{H}(-u + x_j) \right) \quad , \end{aligned}$$

where

$$\mathcal{H}(-a + b) \equiv 1 \text{ if } a \leq b \text{ and } 0 \text{ if } a > b \quad (8)$$

is the Heaviside unit-step function. The system of equations

$$\sum_{j=1}^N w_j \left(1 - \sqrt{1 - 10^{2(u-x_j)}} \mathcal{H}(-u + x_j) \right) = \frac{1}{n} \sum_{i=1}^n \mathcal{I}(u_i \leq u) \quad (9)$$

can be solved in the usual way for $\{w_j\}$ in the case $n = N$ and $\{u_i\} = \{x_j\}$.

The resulting estimates of the natural PDF and CDF of the unprojected quantity (m or r) are $\hat{\mathcal{R}}$ in Eq. (6) and

$$\hat{R}(x) \equiv \sum_{j=1}^N w_j \mathcal{H}(x - x_j) \quad . \quad (10)$$

$\hat{P}(u)$ and $\hat{P}'(u)$ produce *identical* results when evaluated at the sample points $\{u_i\}$. We recognize that they are not estimates but pure transformations of the sample, through the intermediary of the weights $\{w_j\}$. The same is true of $\hat{\mathcal{R}}$ and \hat{R} . They are precise, but not necessarily accurate. We must perform Monte Carlo experiments to determine the accuracy with which $\hat{\mathcal{R}}$ and \hat{R} estimate the true, natural distributions \mathcal{R} and R . We will illustrate how to do this in Sections 4 and 5, using RV results as illustration.

4. RV DATA

To illustrate the methods of Section 3, we studied the sample of the 308 values of $\log m \sin i$ from RV observations at exoplanets.org on 20 October 2010. The sample is listed in Table 1. We followed the procedure of Section 3: we computed the empirical CDF $\hat{P}(m \sin i)$ using Eq. (3); we constructed the system of 308 equations in Eq. (9); we solved them for weights $\{w_j\}$; and we verified that $\hat{P}'(m \sin i)$ from the last line of Eq. (7) was exactly equal to $\hat{P}(m \sin i)$ when evaluated at each value of $\log m \sin i$ in the sample.

The unprojected PDF $\hat{\mathcal{R}}(m)$ from Eq. (6), and the unprojected CDF $\hat{R}(m)$ from Eq. (10), are a bit spiky, due both to the delta and step functions and to the fact that some weights $\{w_j\}$ are negative. Therefore, in Figs. 1–2, we have smoothed $\hat{\mathcal{R}}(m)$ by convolution with a Gaussian with $\sigma = 0.105$ in the logarithm, which is just enough to ensure that $\hat{\mathcal{R}}(m)$ is everywhere non-negative, and that therefore $\hat{R}(m)$ computed from $\hat{\mathcal{R}}(m)$ using Eq. (5) has non-negative slope everywhere.

The results in Figs. 1–2 show that the effect of projection is modest but noticeable. The observed distribution of the projected quantity is shifted to smaller values, as compared with the true distribution, by an amount of ~ 0.08 in the logarithm, or by a $\sim 20\%$ factor in mass.

5. RANDOM DEVIATES

The minimal smoothing of $\hat{\mathcal{R}}(m)$ discussed in Section 4 ensures that the random deviate for m :

$$\mathbb{M} = m\text{-root} \left(\int_{-\infty}^m \hat{\mathcal{R}}(m') dm' = \mathbb{R} \right) \quad (11)$$

is well-defined. Here, \mathbb{R} is the uniform random deviate on the range 0–1. The “ m -root” is defined as value of m that satisfies the equation in parenthesis. The root is found by numerical methods in the usual way.

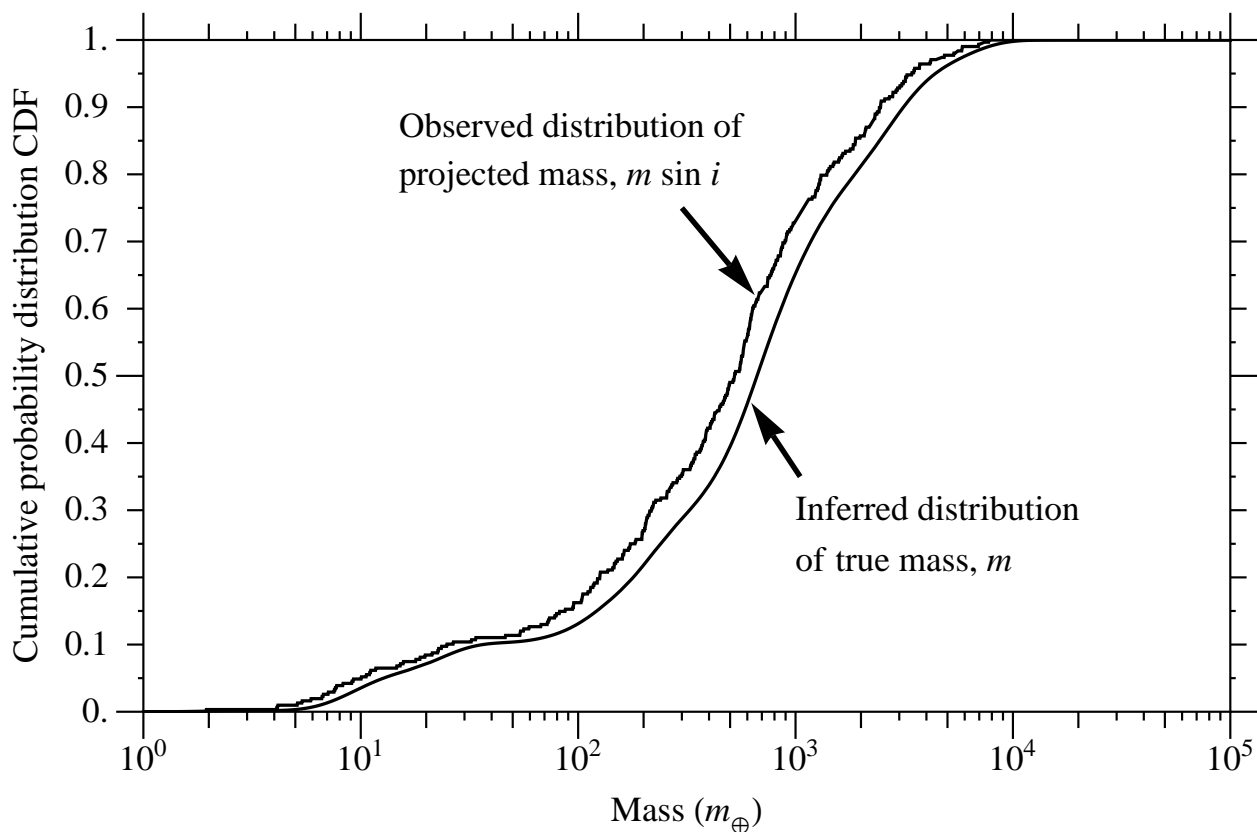


Fig. 1.— Right: the inferred CDF of true exoplanet mass, slightly smoothed. Left: the empirical CDF of 308 RV values of projected mass $m \sin i$. The projected distribution is shifted to the left, due to the distribution of the unknown random factor $\sin i$, by ~ 0.08 in the logarithm, or by a $\sim 20\%$ factor in mass.

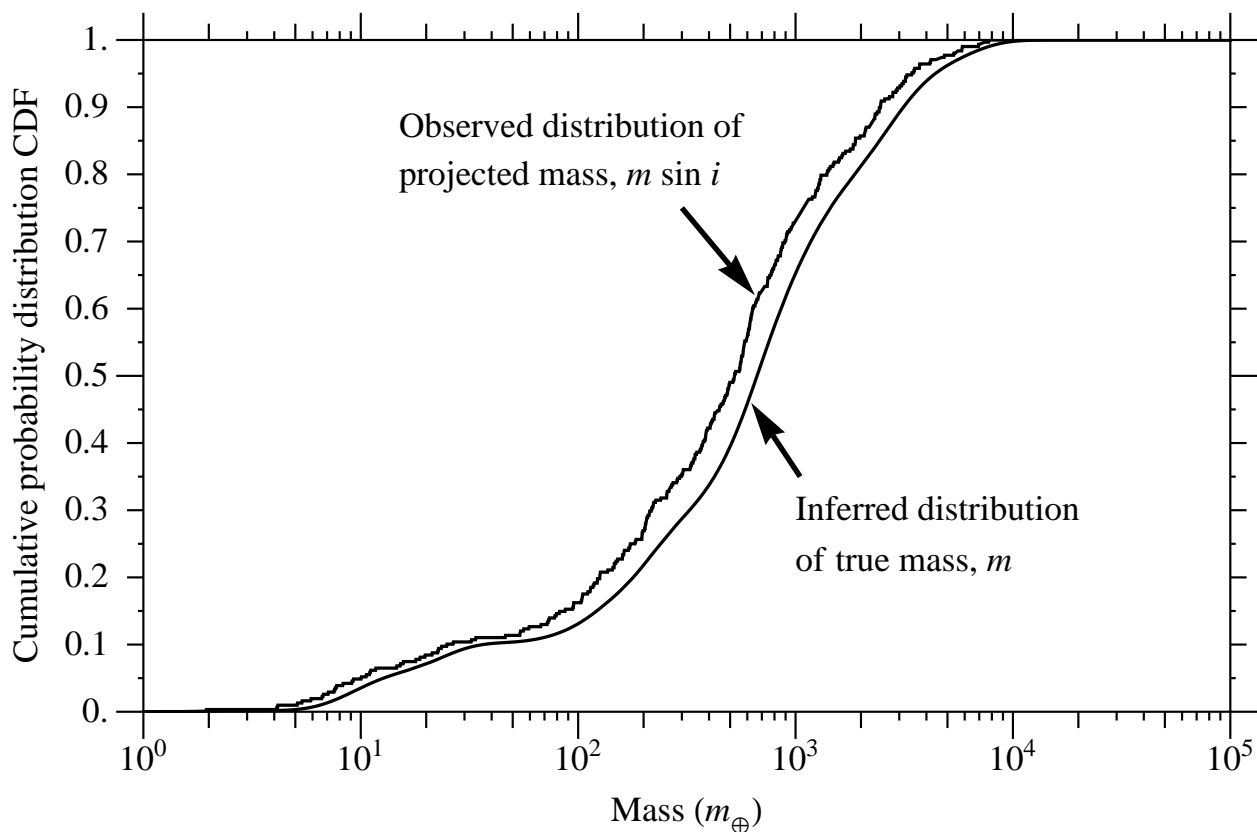


Fig. 2.— Histogram: the 388 RV values of projected mass, $m \sin i$, in bins of 0.05 of the logarithm, expressed as a PDF. Line: the smoothed, inferred PDF of m , the true mass. The projected distribution is shifted to the left, due to the distribution of the unknown random factor $\sin i$, by ~ 0.08 in the logarithm, or by a $\sim 20\%$ factor in mass.

It is a simple matter to show from Eq. (1) that the random deviate for $\sin i$ is

$$\mathbb{S} = \sqrt{2\mathbb{R} - \mathbb{R}^2} \quad . \quad (12)$$

We can combine these results to obtain the random deviate

$$\mathbb{U} \equiv \log(10^{\mathbb{M}}\mathbb{S}) \quad (13)$$

to prepare new samples of $m \sin i$.

To illustrate the usefulness of the random deviate in Eq. (13), we used it to prepare a sample of 1,000,000 values of $m \sin i$, shown in the histogram in Figure 3. We see the modest shift in the projected values referred to in Figures 1 and 2. We also see that the main features in the inferred distribution of true mass, though blurred by \mathcal{Q} , are easily recognizable in this very large sample of projected values generated by the random deviate.

6. ACCURACY

Is the structure in Figure 3 real? This rhetorical question lies at the heart of analyses and science metrics for RV or ML based on the methods in this paper. Monte Carlo experiments using the random deviate in Eq. (13) afford answers to such questions.

To illustrate, we adopt the hypothesis that the structure is true. We ask if we could would recognize the features reliably in the universe of samples of new values of $m \sin i$ generated from Eq. (13). We see in Figures 4–6 that the answer depends on the cardinality of the new samples. For samples of 308 values, we see that the main structural features of the “real” PDF are barely recognizable in the new samples. This means that if the PDF inferred from the sample of 308 values *were* the true distribution in nature, then samples of 308 values would not be expected to reliably detect its principle features. For 1000 values of $m \sin i$, the features are marginally recognizable in each realization. For 100 values—forget about it!

For another example, we treat the sample of 67 RV measurements of Jorissen et al. (2001), kindly provided by A. Jorissen. The inferred distribution of true mass in Figure 7 shows the same potentially believable features as in the earlier treatment (Fig. 2 of Jorissen et al. 2001), particularly the three peaks at about 4, 7.4, and 16 m_J —plus the feature Jorissen et al. found most striking: the minimum between the second and third peaks, in the range 10–13 m_J . They applied a “jackknife” test and concluded this minimum was a “robust result, not affected by the uncertainty in the solution.” If the true distribution had these features, Figure 7 shows that samples of 67 values could not be expected to detect

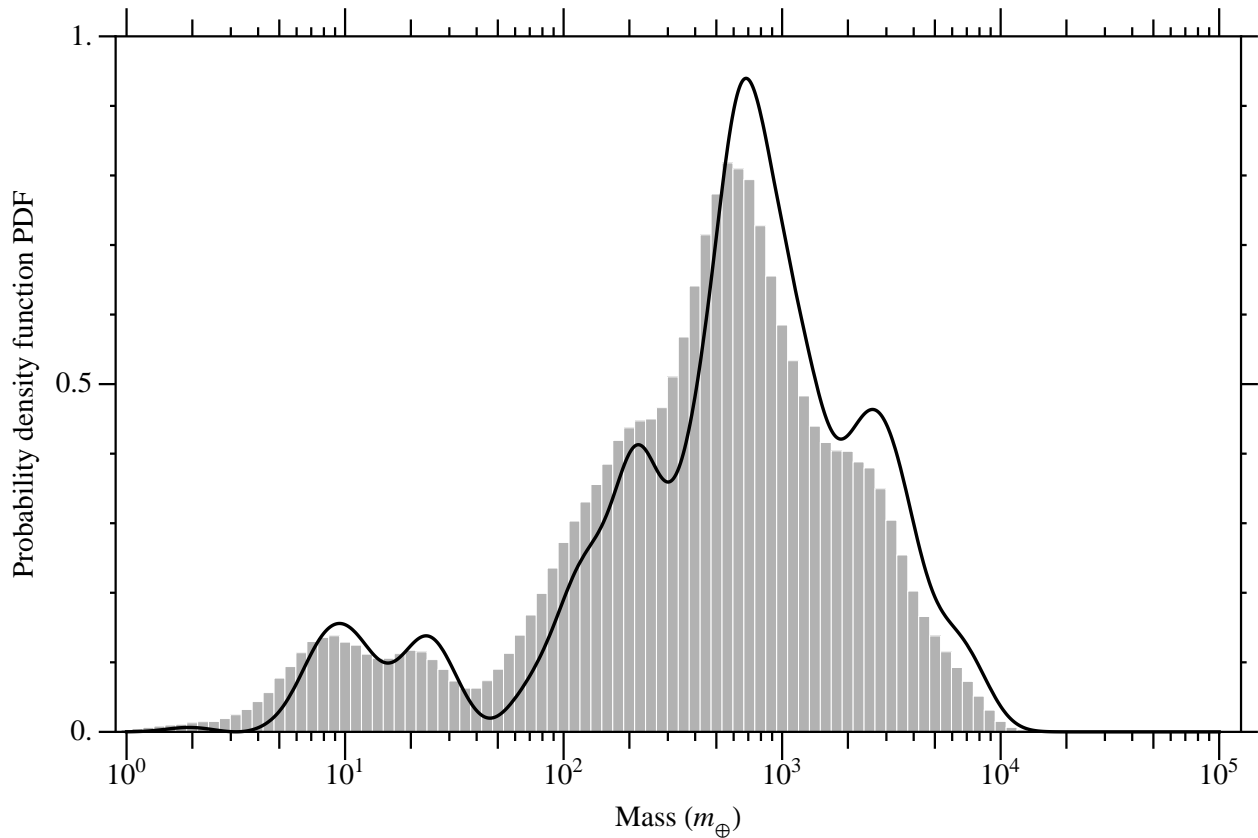


Fig. 3.— Histogram of a sample of 1,000,000 values of $m \sin i$ generated by the random deviate based on the RV sample of 308 values. The slightly smoothed, inferred PDF of true mass m is shown for comparison. Logarithmic convolution with the PDF of $\sin i$, \mathcal{Q} , has shifted the histogram to $\sim 20\%$ lower values and blurred the features in the inferred PDF.

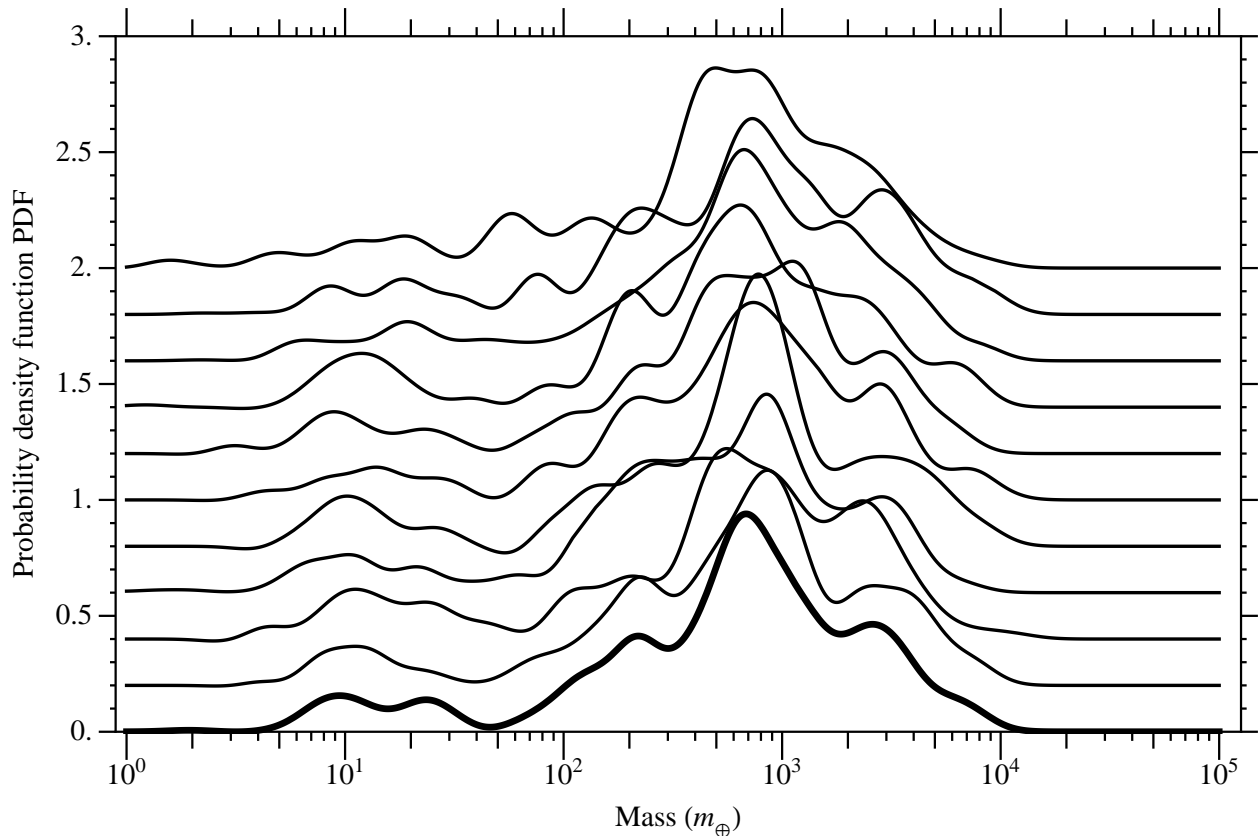


Fig. 4.— Inferred PDFs from 10 new samples of 308 measurements, displaced vertically by steps of 0.1 in density. Each new sample was run through the new computations in Section 3. The bold line is the “real” PDF inferred from the RV data, which is the basis for the random deviate that produced the new samples. For samples of 308 values, we see that the main structural features of the “real” PDF are barely recognizable in the new samples.

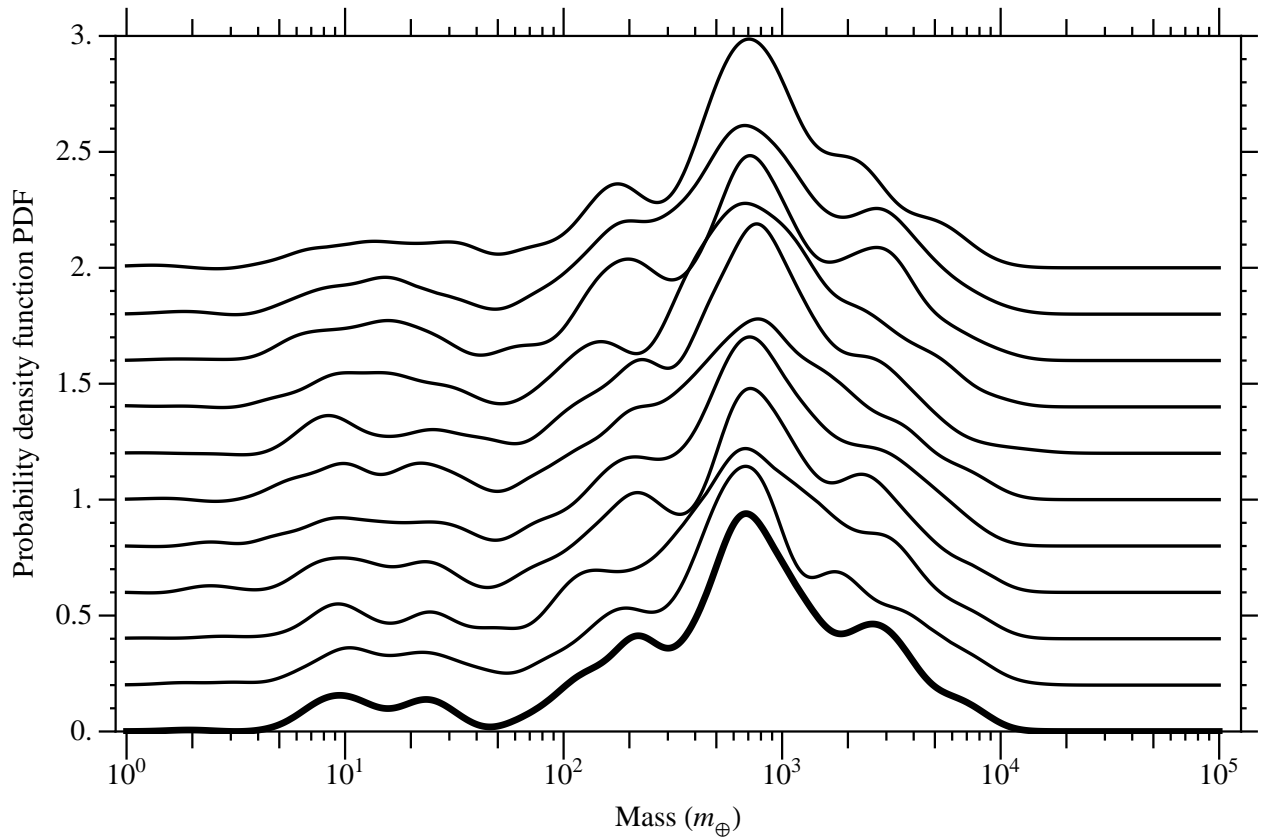


Fig. 5.— PDFs inferred from ten new samples of 1000 values of $m \sin i$. The features in the random deviate (“real” PDF) are marginally recognizable.

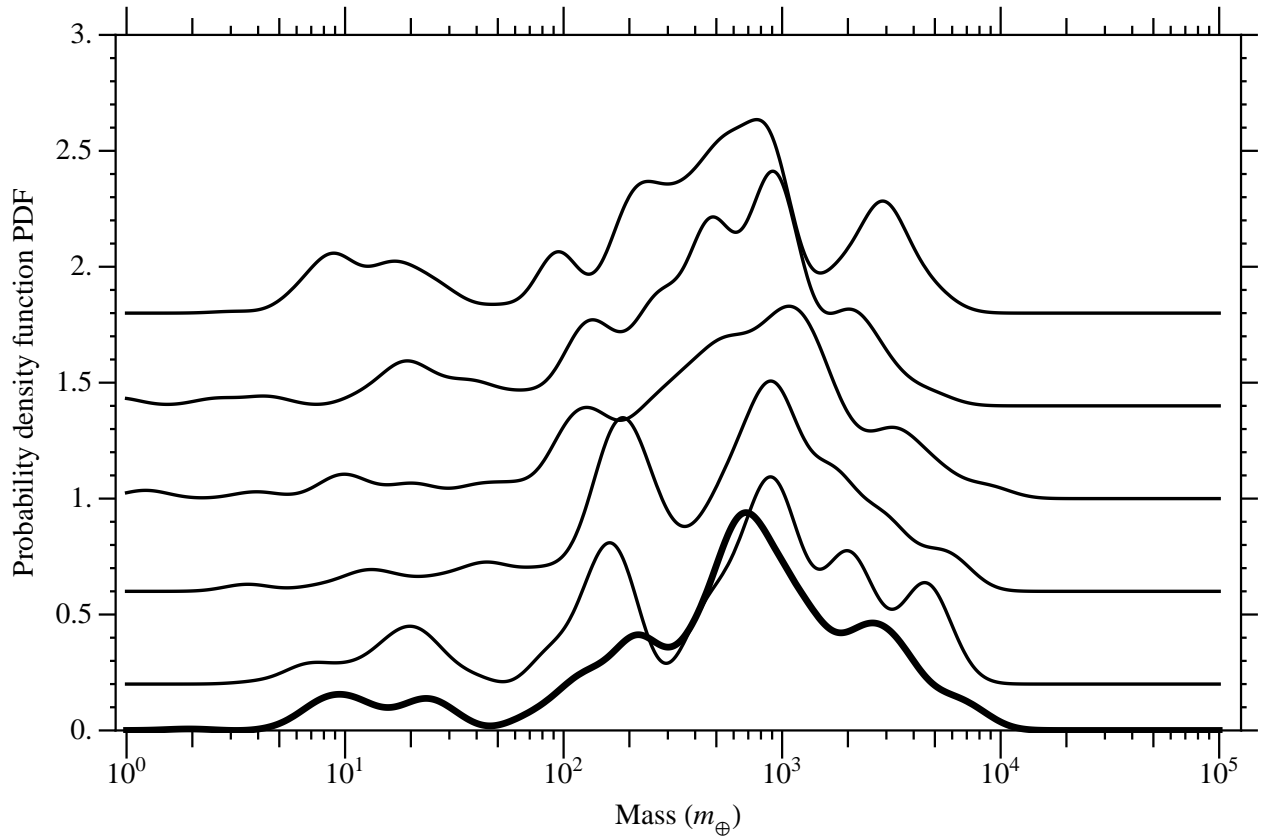


Fig. 6.— PDFs inferred from five new samples of 100 values of $m \sin i$. The statistical noise overwhelms features present in the random deviate.

them with confidence. On the other hand, Figure 8 shows that samples of 2000 values will reliably detect them.

7. COMMENTS AND FUTURE DIRECTIONS

Our treatment of the RV samples is a purely technical demonstration of the methods described in Section 3. While we have accurately characterized the shift due to projection—which would occur in any RV or ML program when the projection angle is unknown, we have neglected selection and systematic effects that must surely be at work in the RV samples.

The methods in this paper offer a basis for better understanding the ability to draw statistical inferences and conclusions about the underlying distribution of true quantities from samples of projected measurements. For example, we see that ability to confidently recognize real features in the distribution should depend only on (1) the scale of the variations compared with the (fixed) blurring scale of \mathcal{Q} in Eq. (1) (i.e., a half-width of $1/\sqrt{5}$ in the logarithm), (2) the amplitude of the features, and (3) the cardinality n of the sample from which the PDF has been computed, which is the only factor under the control of the observer.

For both RV and ML, we envision science metrics developed from double-blind, Monte Carlo experiments using the random deviates derived in this paper. For example, our simple experiments with RV samples suggest that samples of thousands of observed values of a projected quantity may be needed for believable conclusions about the shape features or characteristics of the true distribution.

Great care must be given to incompleteness, systematic effects, and biases, all of which can reduce the fidelity with which a sample of projected values reflects the true distribution of the *projected* quantity. For example, in the case of RV, we know that detection efficiency—and therefore completeness—decreases to zero as the projected mass—and therefore signal-to-noise ratio at the signal threshold decreases. Also, the least-squares estimator for mass from astrometry is known to be biased at low signal-to-noise ratio, and the same can be expected for $m \sin i$ from RV. (Brown 2009; see also Hogg et al. 2010) Any such factors affecting LML samples will bear close scrutiny.

With regard to the ML program recommended by Astro 2010, we anticipate the development of science requirements that define characteristics in the PDF for r that must be recognized or ruled out by the measurements, and with what level of confidence. Monte Carlo experiments can help derive the implied measurement requirements—particularly the cardinality of the sample—that will be needed to satisfy such science requirements.

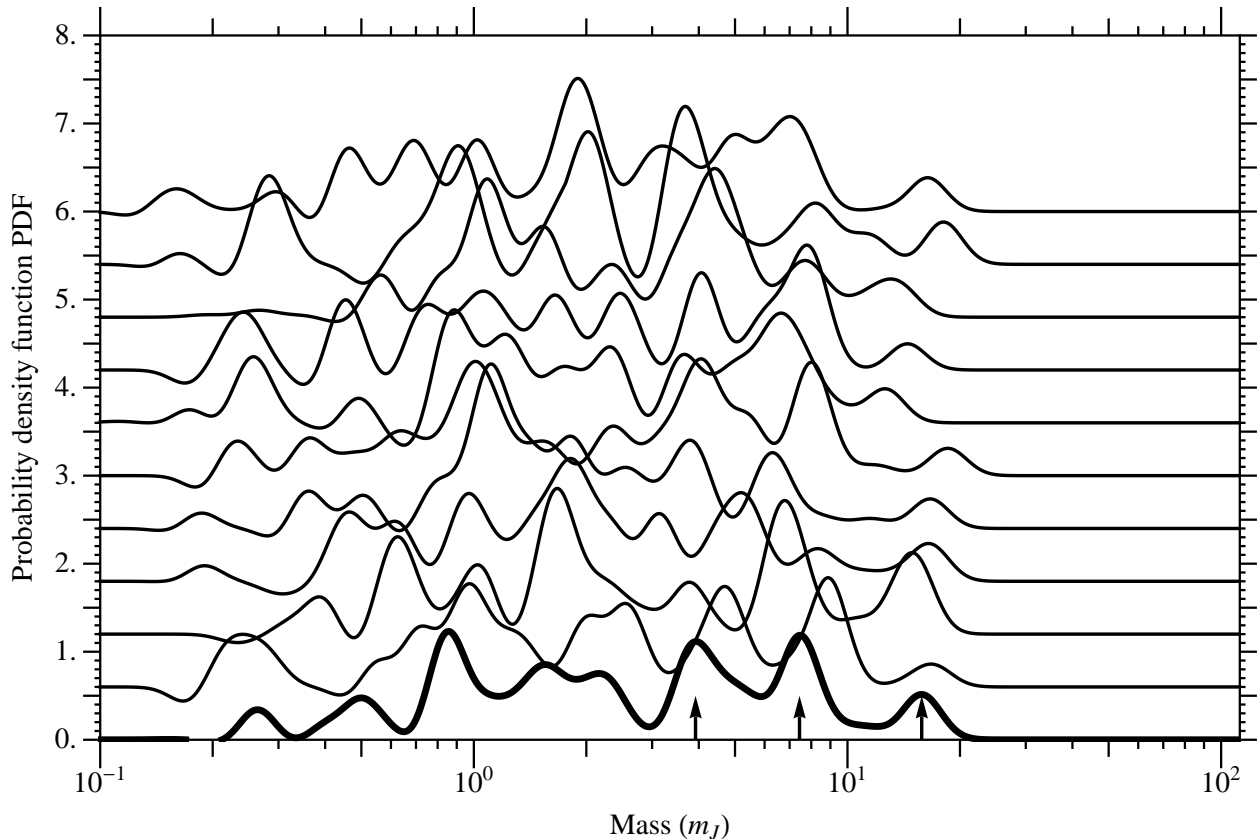


Fig. 7.— Bold: the PDF inferred from the sample of 67 RV measurements of $m \sin i$ used by Jorissen et al. (2001). The PDF has been slightly smoothed, by a Gaussian with $\sigma = 0.05$ in the logarithm. The three peaks indicated by arrows were considered by Jorissen et al. to be at least potentially believable. On the basis of a jackknife test, Jorissen et al. found the minimum between the second and third peaks ($10\text{--}13 m_J$) to be “robust.” The other curves in this figure are random PDFs inferred from new random samples of 67 RV measurements, each produced by the random deviate in Eq. (13), based on the original sample. Each new sample is statistically identical to the original sample. The curves have been displaced upwards by multiples of 0.6 to make them more distinct. Conclusion: if we assumed the distribution in nature were equal to the PDF inferred from the Jorissen sample, then we could not expect any sample of 67 values to reliably detect them.

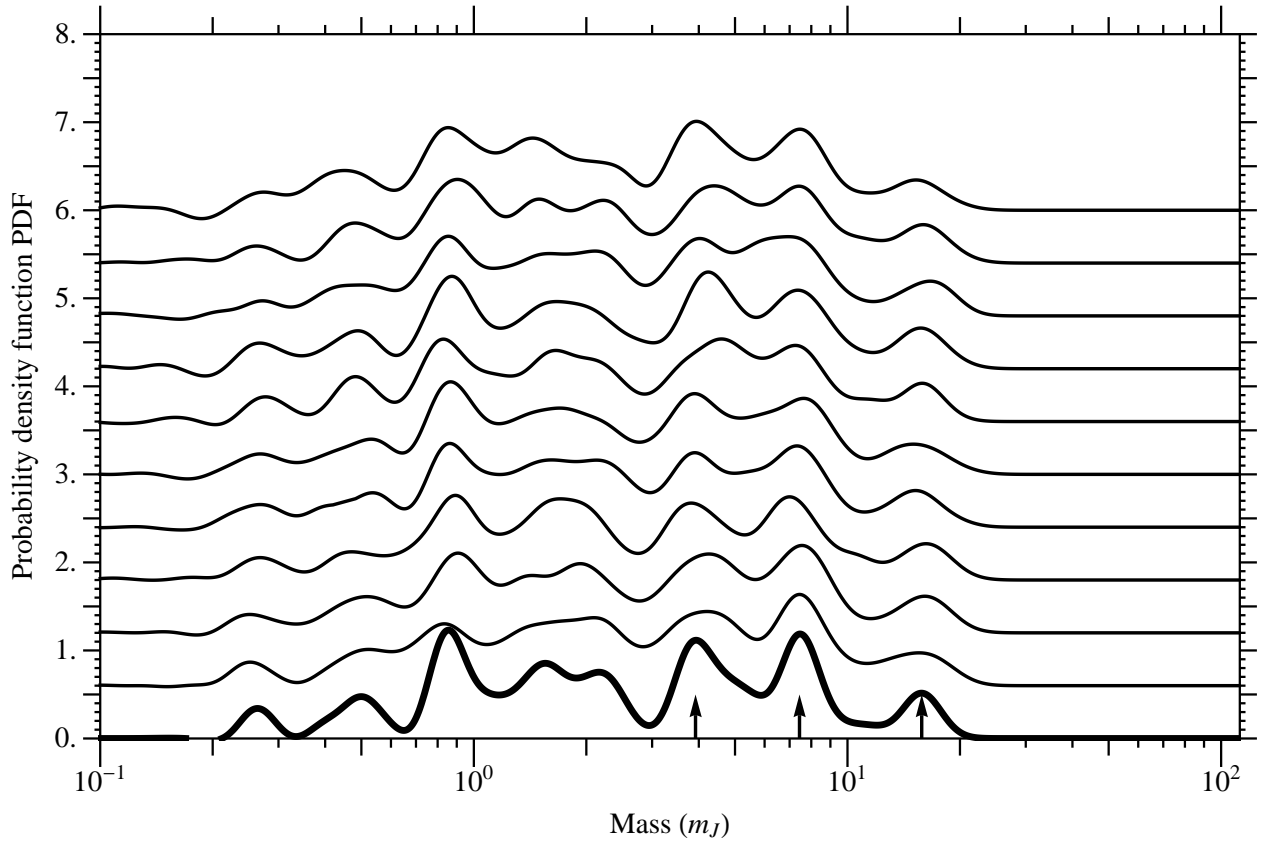


Fig. 8.— Same as Figure 7 except that the new random samples contain 2000 values. All the feature of the Jorissen et al. sample are readily detected.

We thank D. Latham, D. Spiegel, and W. Traub for their helpful comments. We thank A. Jorissen for providing the sample of 67 RV measurements of $m \sin i$ used in Jorissen et al. (2001). We thank Sharon Toolan for her expert preparation of the manuscript.

REFERENCES

- Bennett, D. P., Anderson, J., Beaulieu, J.-P., Bond, I., Cheng, E., Cook, K., Friedman, S., Gaudi, B. S., Gould, A., Jenkins, J., Kimple, R., Lin, D., Mather, J., Rich, M., Sahu, K., Sumi, T., Tenerelli, D., Udalski, A., Yock, P. 2009, arXiv:0902.3000v1
- Blandford, R. D., & Committee for a Decadal Survey of Astronomy and Astrophysics 2010, “New Worlds, New Horizons in Astronomy and Astrophysics,” (National Academies Press: Washington, D.C.)
- Brown, J. R., & Harvey, M. E. 2007, *Journal of Statistical Software*, 19, 1
- Brown, R. A. 2009, *ApJ*, 699, 711
- Chandrasekhar, S., & Münch, G. 1950, *ApJ*, 111, 142
- Durban, J. 1968, *The Annals of Mathematical Statistics*, 39, 398
- Glen, A. G., Leemis, L. M., & Drew, J. H. 2004, *Computational Statistics and Data Analysis*, 44, 451
- Hogg, D. W., Myers, A. D., & Bovy, J. 2010, arXiv:1008.4146v2
- Jorissen, A., Mayor, M., & Udry, S. 2001, *A&A*, 379, 992

Table 1. The 308 Values of $m \sin i$ from RV at exoplanets.org on 20 October 2010

Exoplanet	$m \sin i (R_{\oplus})$	Exoplanet	$m \sin i (R_{\oplus})$	Exoplanet	$m \sin i (R_{\oplus})$
GJ 581 e	1.943	HD 45364 b	59.490	47 UMa c	173.489
HD 40307 b	4.103	HD 107148 b	67.444	HD 175541 b	182.742
HD 156668 b	4.151	HD 46375 b	72.222	HIP 14810 d	184.560
61 Vir b	5.110	HD 3651 b	72.786	HD 27894 b	196.424
GJ 581 c	5.369	HD 76700 b	73.793	HD 11964 b	196.508
GJ 876 d	5.893	HD 168746 b	77.913	GJ 876 c	196.761
HD 215497 b	6.629	HD 16141 b	79.359	HD 330075 b	198.268
HD 40307 c	6.722	HD 108147 b	82.012	HD 37124 d	202.306
GJ 581 d	7.072	HD 109749 b	87.311	HD 192263 b	203.245
HD 181433 b	7.544	HIP 57050 b	94.643	HD 181433 c	203.574
HD 1461 b	7.630	HD 101930 b	95.105	GJ 832 b	204.802
55 Cnc e	7.732	HD 88133 b	95.187	HD 216770 b	205.644
GJ 176 b	8.264	GJ 649 b	103.419	HD 37124 b	206.867
HD 40307 d	9.100	HD 215497 c	104.113	HD 45364 c	209.326
HD 7924 b	9.256	BD –08 2823 c	104.296	HD 170469 b	212.557
HD 69830 b	10.060	HD 33283 b	104.954	<i>v</i> And b	212.747
61 Vir c	10.609	HD 47186 c	110.712	HD 96167 b	217.609
μ Ara d	10.995	HD 164922 b	113.777	HD 209458 b	218.862
GJ 674 b	11.087	HD 149026 b	114.129	HD 37124 c	221.403
HD 69830 c	11.689	HD 93083 b	117.035	HD 9446 b	222.123
BD –08 2823 b	14.604	HD 181720 b	118.247	HD 224693 b	227.153
HD 4308 b	15.175	HD 63454 b	122.451	HD 34445 b	239.582
GJ 581 b	15.657	HD 126614 A b	122.607	HD 187085 b	255.476
HD 69830 d	17.908	HD 83443 b	125.835	HD 134987 c	255.868
HD 190360 c	18.746	HD 212301 b	125.927	HD 4208 b	256.672
HD 219828 b	19.778	HD 6434 b	126.259	GJ 179 b	262.008
HD 16417 b	21.285	BD –10 3166 b	136.656	GJ 849 b	263.683
HD 47186 b	22.634	HD 102195 b	143.935	55 Cnc b	268.236
61 Vir d	22.758	HD 75289 b	146.236	HD 38529 b	272.456
GJ 436 b	23.490	51 Peg b	146.587	HD 155358 b	284.379
HD 11964 c	24.905	HD 45652 b	148.909	HD 179949 b	286.749
HD 179079 b	26.631	HD 2638 b	151.731	HD 10647 b	294.048
HD 49674 b	32.287	HD 155358 c	160.167	HD 114729 b	300.317
HD 99492 b	33.752	HD 99109 b	160.273	HD 185269 b	303.322
55 Cnc f	46.285	HD 187123 b	162.135	HD 154345 b	304.180
HD 102117 b	53.962	HD 208487 b	162.817	HD 108874 c	326.896
55 Cnc c	54.254	HD 181433 d	170.218	HD 60532 b	328.940

Table 1—Continued

Exoplanet	$m \sin i (R_{\oplus})$	Exoplanet	$m \sin i (R_{\oplus})$	Exoplanet	$m \sin i (R_{\oplus})$
HD 117618 b	56.154	μ Ara e	172.710	HD 130322 b	331.575
ρ CrB b	338.250	16 Cyg B b	521.310	HD 147018 b	676.160
HD 52265 b	340.571	HD 167042 b	522.435	HD 118203 b	679.059
ϵ Eri b	344.932	HD 4113 b	523.954	HD 216437 b	689.212
HD 231701 b	345.428	HD 142415 b	528.293	HD 206610 b	707.519
HD 114783 b	351.270	HD 82943 b	551.047	HD 212771 b	715.885
HD 189733 b	362.504	HD 50499 b	554.610	HD 202206 c	740.966
HD 73534 b	367.323	μ Ara b	554.861	HD 154857 b	741.503
HD 100777 b	370.334	HD 87883 b	558.101	HD 12661 b	744.088
GJ 317 b	373.522	HD 20782 b	560.637	HD 4313 b	746.348
HD 147513 b	374.984	γ Cep b	563.066	HD 192699 b	758.958
HD 48265 b	383.503	HD 89307 b	563.295	HD 73526 c	769.550
HD 148427 b	385.455	HD 68988 b	572.154	HD 23079 b	776.670
HD 216435 b	386.126	HD 74156 b	573.902	HD 60532 c	782.970
HD 65216 b	386.653	HD 8574 b	574.096	HD 43691 b	793.794
HD 121504 b	388.542	HD 9446 c	577.1001	HD 75898 b	799.475
HD 95089 b	392.849	HD 117207 b	578.187	47 UMa b	809.281
HD 210277 b	404.579	HD 171028 b	581.417	HD 41004 A b	812.705
HIP 14810 c	405.351	HD 45350 b	583.668	HD 171238 b	829.345
HD 108874 b	410.126	HD 73256 b	594.119	HD 217107 c	831.396
HD 142 b	415.053	HD 13931 b	598.001	HD 62509 b	854.159
HD 19994 b	421.763	μ Ara c	600.493	HD 164604 b	854.614
HD 149143 b	422.815	HD 190647 b	604.908	HD 81688 b	855.313
HD 30562 b	423.584	HD 70642 b	606.968	11 Com b	864.016
HD 114386 b	433.490	ν And c	609.864	HD 153950 b	871.649
HD 217107 b	445.384	GJ 876 b	614.349	HD 66428 b	874.042
HD 23127 b	446.577	HD 5319 b	615.961	ξ Aql b	892.158
HIP 5158 b	453.398	HD 187123 c	617.382	HD 196050 b	903.853
HD 128311 b	463.211	HD 12661 c	619.448	HD 73526 b	907.731
HD 188015 b	467.143	HD 210702 b	624.623	HD 37605 b	908.618
HD 205739 b	472.709	HD 5388 b	624.658	HD 169830 b	918.494
HD 86081 b	475.529	κ CrB b	629.334	HD 196885 b	935.799
BD +14 4559 b	482.948	HD 82943 c	632.344	HD 181342 b	953.480
HD 177830 b	487.061	HD 136418 b	633.689	HD 143361 b	964.755
HD 190360 b	487.980	HD 20868 b	638.619	HD 73267 b	973.522
ϵ Ret b	491.944	ι Hor b	650.641	HD 221287 b	990.300
HD 180902 b	494.977	6 Lyn b	657.736	HD 72659 b	1003.123

Table 1—Continued

Exoplanet	$m \sin i(R_{\oplus})$	Exoplanet	$m \sin i(R_{\oplus})$	Exoplanet	$m \sin i(R_{\oplus})$
HD 134987 b	496.992	HD 4203 b	661.869	HD 17156 b	1024.490
HD 159868 b	516.287	HIP 79431 b	671.672	HD 128311 c	1032.619
HD 32518 b	1063.456	14 Her b	1651.132	γ Leo A b	2802.989
HD 1237 b	1072.773	81 Cet b	1697.742	ι Dra b	2803.565
HD 183263 c	1105.088	HD 132406 b	1781.687	HD 33564 b	2901.538
HD 125612 b	1119.434	HD 145377 b	1837.971	HD 33636 b	2946.568
HD 92788 b	1132.890	HD 28185 b	1842.802	HD 141937 b	3011.953
HD 183263 b	1136.237	HD 102272 b	1879.590	HD 30177 b	3079.540
HD 195019 b	1137.966	HD 2039 b	1883.421	30 Ari B b	3139.968
HD 190984 b	1190.820	HD 190228 b	1888.806	HD 139357 b	3202.743
HIP 14810 b	1231.588	HD 10697 b	1981.982	HD 39091 b	3206.748
HD 80606 b	1236.588	HD 11977 b	2072.545	18 Del b	3245.402
42 Dra b	1237.297	HD 104985 b	2082.307	HD 38801 b	3420.489
55 Cnc d	1261.592	HD 147018 c	2095.941	HD 156846 b	3499.068
GJ 86 b	1271.840	HD 86264 b	2106.695	11 UMi b	3524.403
HD 40979 b	1278.579	HD 81040 b	2185.897	HD 136118 b	3713.095
HD 169830 c	1291.466	HD 111232 b	2200.074	HD 114762 b	3713.985
HD 204313 b	1291.660	HD 106252 b	2212.151	HD 38529 c	4157.806
ν And d	1308.326	4 UMa b	2267.236	BD +20 2457 c	4187.622
τ Boo b	1309.541	HD 240210 b	2316.907	HD 16760 b	4577.149
HD 16175 b	1392.132	HD 178911 B b	2317.730	HD 162020 b	4836.124
HD 50554 b	1398.267	70 Vir b	2371.824	HD 202206 b	5348.098
HD 142022 b	1420.156	ϵ Tau b	2422.334	HD 168443 c	5572.360
HD 213240 b	1440.776	HD 222582 b	2425.415	HD 131664 b	5826.122
14 And b	1488.884	HD 23596 b	2461.236	HD 41004 B b	5853.237
HD 11506 b	1505.054	HD 168443 b	2465.680	HD 137510 b	6936.118
HD 17092 b	1577.327	HD 175167 b	2472.565	BD +20 2457 b	7207.109
HD 154672 b	1591.415	HD 74156 c	2572.856	HD 43848 b	7729.763
HIP 2247 b	1628.547	HD 89744 b	2693.210		